Available online at www.sciencedirect.com
SCIENCE DIRECT®
Journal of Magnetic Resonance 165 (2003) 208–218
JMR Journal of Magnetic Resonance
www.elsevier.com/locate/jmr

Fast-MAS total through-bond correlation spectroscopy using adiabatic pulses

Edme H. Hardy,[1] Andreas Detken, and Beat H. Meier*

Physical Chemistry, ETH Hoenggerberg, CH-8093 Zurich, Switzerland

Received 21 May 2003; revised 7 August 2003

Communicated by Lucio Frydman

Abstract

Pulse sequences consisting of adiabatic pulses for total through-bond correlation spectroscopy (TOBSY) under magic-angle spinning (MAS) are introduced. Above a certain threshold, the polarization transfer achieved with these sequences is largely insensitive to the amplitude and homogeneity of the radiofrequency field employed. An experimental transfer efficiency of up to 76% was achieved in a two-spin system using the sequence $WiW9^{1}_{24}$ at a MAS frequency of 26.67 kHz. Applications to resonance assignments in the dipeptide L-Val–L-Phe and in the cyclic decapeptide antamanide are demonstrated.

Keywords: Solid-state NMR; MAS; Polarization transfer; Total correlation spectroscopy; TOBSY; Adiabatic pulses; Assignment

1. Introduction

In solid-state NMR, coherent polarization transfer between spins can be either mediated by dipole–dipole couplings, which act "through space," or by the indirect (J) coupling, which acts "through bonds." Both mechanisms can be employed for total-correlation spectroscopy [1]. Here, we introduce novel "total through-bond correlation spectroscopy" (TOBSY) experiments [2] based on adiabatic pulses.

In the TOBSY experiment, a radiofrequency (RF) pulse sequence is applied that ideally creates a pure isotropic J-coupling average Hamiltonian. Under magic-angle spinning (MAS), attention must be paid that this pulse sequence does not reintroduce undesired interactions which are otherwise averaged by the MAS rotation, in particular, dipolar interactions and the anisotropic part of the chemical shift (CSA). Such undesired recoupling can be avoided by using specifically designed rotor-synchronized pulse sequences. These sequences often require a fixed ratio of the RF amplitude (expressed as a nutation frequency, in kHz, of the spins to which the RF is applied) to the MAS frequency. This limits not only the range of MAS frequencies at which a given sequence can be applied, but also renders the performance of the pulse sequence susceptible to RF inhomogeneity and missettings of the pulse amplitude. Specifically, the first TOBSY sequence [2] was limited to MAS frequencies below about 5 kHz for practically achievable RF amplitudes.

In recent years, symmetry principles have been introduced which allow one to conveniently analyze two classes of rotor-synchronized sequences, the so-called CN^{v}_{n} and RN^{v}_{n} sequences (see, e.g. [3]). Based on these principles, we [4] and others [5] have proposed a set of TOBSY sequences of the type CN^{v}_{n} which can be applied over a wide range of MAS frequencies. Specifically, sequences of the type $P9^{1}_{n}$, which use the POST element [6] as a basic RF cycle ('C element'), were evaluated. More recently, the use of the sequence $R30^{14}_{6}$ was proposed and demonstrated experimentally [7]. Also these sequences require the RF amplitude to be a certain multiple of the MAS frequency and are susceptible to RF inhomogeneity. The tolerance of the sequence to RF missettings generally depends on the type of sequence

* Corresponding author. Fax: +41-1-632-1621.
E-mail address: beme@ethz.ch (B.H. Meier).
[1] Present address: Institut für Mechanische Verfahrenstechnik und Mechanik, Universität Karlsruhe, D-76128 Karlsruhe, Germany.

1090-7807/$ - see front matter © 2003 Elsevier Inc. All rights reserved.
doi:10.1016/j.jmr.2003.08.003

and on the type of (composite) pulse used as a basic RF element. Specifically, it has been predicted that the sequence $R30_6^{14}$ is more tolerant to RF missettings than the $P9_n^1$ sequences [7].

In this paper, we show that the influence of RF missettings or inhomogeneity can be much reduced by using adiabatic inversion pulses for constructing CN_n^v sequences. Adiabatic pulses can achieve an inversion of single-spin polarization for a wide range of RF amplitudes as long as the adiabatic condition is fulfilled. If such pulses are used for constructing a TOBSY sequence, the ratio of the RF amplitude to the MAS frequency is no longer fixed.

The use of adiabatic pulses for isotropic mixing was first introduced in the context of ^1H–^1H TOCSY in liquid-state NMR [8] and was later extended to ^{13}C–^{13}C transfer [9] and to magic-angle spinning of liquids [10]. The pulse sequences used in liquids are, however, generally not applicable to solids. For solid systems, the use of adiabatic inversion pulses has been proposed and evaluated for rotational-echo double resonance (REDOR) [11,12], for which somewhat different considerations apply than for CN_n^v sequences.

Following the Section 2, criteria for the choice of the parameters for the adiabatic pulses and the C elements are discussed. The proposed sequences are then analyzed in simulations and characterized in experiments. Finally, we will show two applications to assignment in biomolecular systems.

2. Materials and methods

2.1. Materials

[2,3-$^{13}C_2$]Sodium propionate, [U-$^{13}C_2$]zinc acetate, and [U-^{13}C,^{15}N]L-Val–L-Phe dipeptide were purchased from Cambridge Isotopes Laboratories. [U-^{13}C,^{15}N]Antamanide was kindly obtained from Prof. M. Kainosho, Dr. T. Kawakami, and Prof. S. Aimoto and recrystallized as described in [13].

2.2. NMR

Experiments were carried out at a static field of 14.09 T on a Bruker AV600 spectrometer, equipped with a 2.5-mm double-resonance probe. The MAS frequency was actively stabilized to within ±5 Hz.

For one-dimensional (1D) exchange experiments on the two-spin systems of sodium propionate and zinc acetate, initial ^{13}C coherence was created by APHH cross-polarization from the protons [14]. For the experiments on sodium propionate, a DREAM double-quantum spin-pair filter [15,16] was additionally applied for ensuring that only those molecules which are doubly labelled are observed. This filter was left away for experiments on zinc acetate. One specific resonance was then selected by setting the RF frequency on-resonance for this resonance, dephasing the other resonance by $\pi/2$ during an evolution period t_1, and applying a Z filter for 2 ms. Subsequently, the RF frequency was set back to the center of the two resonances and the TOBSY mixing sequence using adiabatic pulses was applied. The complete pulse scheme is depicted in Fig. 1.

For two-dimensional (2D) experiments, the frequency switching and the Z filter were omitted. The ^{13}C transmitter frequency was set to 95 ppm, which is approximately the center of the chemical shift range of both molecules studied. Spectra were acquired with the spectral width in the indirect dimension set to 50 kHz, using the TPPI scheme.

For execution of the $WiW9_n^1$ mixing sequence, the amplitude and phase functions of each inversion pulse were discretized into time steps of 400 ns. The correct execution of the pulse sequence was carefully verified with a Tektronix TDS7104 digital oscilloscope.

The RF amplitude on the ^{13}C channel was 50 kHz during CP and 80 kHz for the "hard" $\pi/2$ pulses.

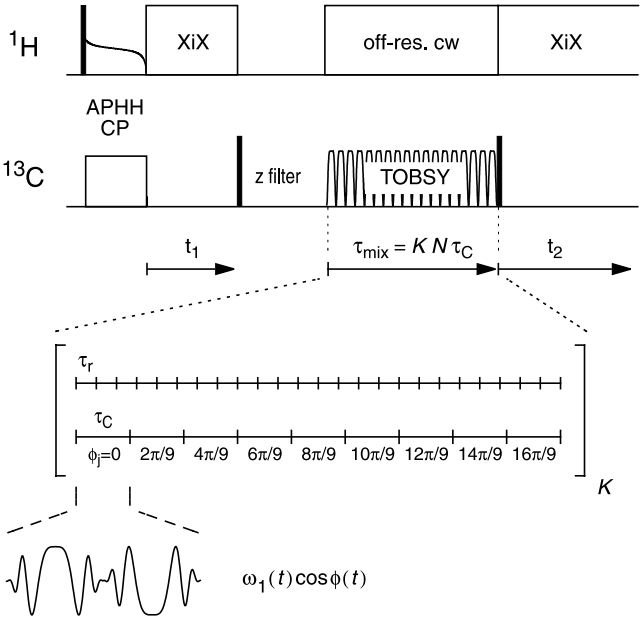

Fig. 1. Pulse scheme for 1D and 2D total through-bond correlation spectroscopy using adiabatic pulses. Filled black rectangles represent $\pi/2$ pulses. Initial transverse carbon polarization is created by cross-polarization via adiabatic passage through the Hartmann–Hahn condition (APHH CP). After the variable evolution period t_1, in the 1D experiments, a Z filter was applied; this filter and the frequency switching were omitted in 2D experiments. The ensuing mixing sequence consists of K supercycles. Each supercycle contains $N = 9$ RF cycles (C elements) synchronized to n rotor cycles, with $n = 9p \pm 3$, p integer. The C elements are constructed from two adiabatic inversion pulses which are phase shifted by π. The x-component of the RF amplitude in a frame rotating with a fixed frequency (the frequency at the center of the sweep) is shown for a typical cycle at the bottom. Successive RF cycles are phase-shifted according the CN_n^v scheme.

The protons were decoupled during the evolution and detection periods using the XiX scheme [17,18] with an RF amplitude of 150 kHz and a pulse length of 106.1 μs. During the adiabatic TOBSY sequence, off-resonance cw decoupling was applied with an RF amplitude of 160 kHz and with an RF offset of 190 kHz.

2.3. Numerical simulations

The single-spin inversion by an amplitude- and phase-modulated pulse as well as the polarization transfer of various TOBSY sequences using such pulses as building blocks were simulated by calculating the evolution of the spin-density operator under a piecewise constant Hamiltonian, using the GAMMA simulation environment [19]. For simulating single-spin inversion, a chemical-shift (CS) anisotropy of 7.5 kHz was assumed. For simulating polarization transfer, a ^{13}C two-spin system with a dipolar coupling constant of 2 kHz and a J coupling of 50 Hz was taken. CS anisotropies of 7.5 kHz and 0.5 kHz and asymmetries of 0.1 and 0.05 were assumed for the two spins, respectively. The two CSA tensors were assumed to be parallel and rotated by $\beta = \pi/2$ with respect to the principal axis system of the dipolar tensor. If not varied, the isotropic chemical shifts were ± 6 kHz. At least 500 time steps per rotor cycle or adiabatic inversion pulse were taken, depending on which duration was shorter. Two hundred crystal orientations [20] were used for the powder average.

3. CN_n^v sequences using adiabatic pulses

3.1. Selection rules

The basic element of a CN_n^v sequence is an RF cycle ('C element') of duration τ_C with unity propagator: $U_{RF}(\tau_C) = \pm 1$. N such RF cycles are synchronized to n rotor periods τ_r, while successive C elements are phase-shifted by $v2\pi/N$, where v is an integer. This pulse sequence interferes with the MAS rotation and can thereby reintroduce spin interactions into the lowest-order average Hamiltonian whose contribution would be zero under MAS alone. Based on the symmetry properties of the different interactions under real-space and spin-space rotations, selection rules have been derived which predict the contributions to the average Hamiltonian that are zero by the combined action of MAS and the pulse sequence [3,21].

The most basic selection rule states that contributions to the lowest-order average Hamiltonian are zero unless

$$mn - \mu v = kN. \tag{1}$$

Here, m takes all integer values between $-l$ and $+l$, where l is the rank of the interaction under real-space rotations. Likewise μ takes all integer values between $-\lambda$ and $+\lambda$, where λ is the rank under spin-space rotations. The integer k can take arbitrary values. This selection rule was initially derived only for C elements that are purely amplitude-modulated [21]. Later, in [3] a general derivation of the average Hamiltonian was given which is valid also for the case of amplitude- and phase-modulated C elements, as are used here.

For a TOBSY sequence, the selection rule Eq. (1) must only be fulfilled for $m = \mu = k = 0$ (i.e., no anisotropic interactions should be recoupled by the pulse sequence). Suitable combinations of N, n, and v that fulfill this requirement were given in [4]. Specifically, if $v = 1$, N must be at least 9, leading to possible TOBSY sequences of the type $C9^1_{9p\pm3}$ with an integer p.

The inevitable contributions from $m = \mu = k = 0$ comprise the isotropic interactions: the (desired) J interaction as well as the (undesired) isotropic chemical shifts. It is exactly this set of interactions which is present to lowest order average Hamiltonian theory (AHT) under MAS alone, *without* applying any pulse sequence. The task of the pulse sequence is to suppress the chemical shifts while retaining the J couplings. This suppression must be achieved by choosing suitable pulses as building blocks for the pulse sequence, while the symmetry of the overall sequence merely ensures that no other interactions are reintroduced. Here, we employ adiabatic inversion pulses for chemical-shift suppression, for which the initial and final states before and after each pulse, respectively, are aligned with the z-axis of the laboratory frame. In the following, we discuss some requirements for these pulses in order to achieve a high transfer efficiency of the overall sequence.

3.2. Adiabatic pulses in CN_n^v sequences

For constructing a C element, we concatenate two adiabatic inversion pulses of length $T_p = \tau_C/2$. The pulses are identical except for an overall phase shift of π for the second pulse. We further impose that the pulse amplitudes and phases are symmetric around the center of each pulse. This ensures that the two-pulse element is antisymmetric with respect to its center:

$$H_{RF}(\tau_C - t) = -H_{RF}(t), \quad 0 \leqslant t < \tau_C. \tag{2}$$

Such a two-pulse element constitutes a proper C element, i.e., the RF propagator of the element is unity. This can be shown by dividing the element into two halves and subdividing the two halves into infinitesimal time steps each in which the Hamiltonian can be regarded as constant. The propagator for the last time step of the first half and the propagator for the first time step of the second half multiply to unity, which by induction leads to unity for the propagator as a whole. Note that at this point we have not made any assumptions about the specific amplitude and phase modulation functions employed apart from the symmetry. The specific form of

the C elements will not affect the selection rules, but only the efficiency of the suppression of the isotropic chemical shifts. While our choice of the C element proves convenient, it is not unique, and other C elements containing adiabatic pulses are conceivable.

Schematic amplitude and phase definitions of the C element, as they would be executed by the spectrometer, are shown in Fig. 2a. The phase (modulo 2π) is the RF phase in a frame rotating with a fixed frequency, called the phase-modulation or PM frame in [22]. The trajectory of the single-spin polarization during a two-pulse element is visualized in Figs. 2b and c. The effective field and the trajectory are sketched in a frame rotating with the RF field in such a way that the phase of the effective field over the course of a single pulse is constant (this frame is called the frequency-modulation or FM frame in [22]). In this frame, the first pulse starts with a positive frequency offset, which adds to the chemical shift to yield an initial effective field along the $+z$-axis (position 1 in Fig. 2b. The adiabatic sweep then takes the effective field (grey arrows) to the $-z$-axis via the positive x-axis. The polarization (black arrows), assumed to be initially along $+z$, follows the effective field. At the sweep center (position 2), the effective field and the polarization still have a positive z component (for a positive shift offset): the polarization is above the x–y-plane for a longer time than below. At the end of the first sweep, the polarization has been completely inverted (position 3). The second sweep is identical to the first except for an overall phase shift of π, which lets the effective field cross the x–y-plane along the $-x$-axis if viewed in the same rotating frame as the first pulse (movement from position 4 via 5 to 6 in Fig. 2c. The polarization is now locked to the negative effective-field direction and moves from 4′ via 5′ to 6′, spending a longer time below the x–y-plane than above. At the end of the RF cycle, the polarization has returned to its initial position.

A large number of adiabatic inversion pulses have been proposed in the literature in the context of liquid-state NMR [23–25]. For the present study, we chose the WURST-q [26] pulse,

$$\omega_1(t) = \omega_1^{\max}\left(1 - |\sin(t\pi/T_p)|^q\right),$$
$$t \in \left[-T_p/2, T_p/2\right], \tag{3}$$

with a constant frequency sweep rate of

$$\ddot{\phi}(t) = (\omega_1^{\max})^2/Q_0. \tag{4}$$

The exponent q determines the shape of the amplitude modulation function; the larger the value of q, the 'flatter' the amplitude shape in the center of the pulse and the sharper the cutoff at the edges. The parameter Q_0 determines the sweep rate for a given maximum RF amplitude $\omega_1^{\max}$.

We call the C element constructed from two such pulses WURST-inverse-WURST or WiW. Nine WiW cycles are concatenated with successive phase shifts of $2\pi/9$ to form a $\mathrm{WiW9}_n^1$ supercycle. Such a supercycle is depicted in the bottom of Fig. 1 for the sequence $\mathrm{WiW9}_{24}^1$.

One criterion for the performance of the pulse sequence is the cycle time. Roughly speaking, for shorter cycle times a smaller contribution of higher-order terms in the average Hamiltonian expansion may be expected. For achieving a short cycle time, it is desirable to keep the individual inversion pulses as short as possible without compromising the inversion efficiency.

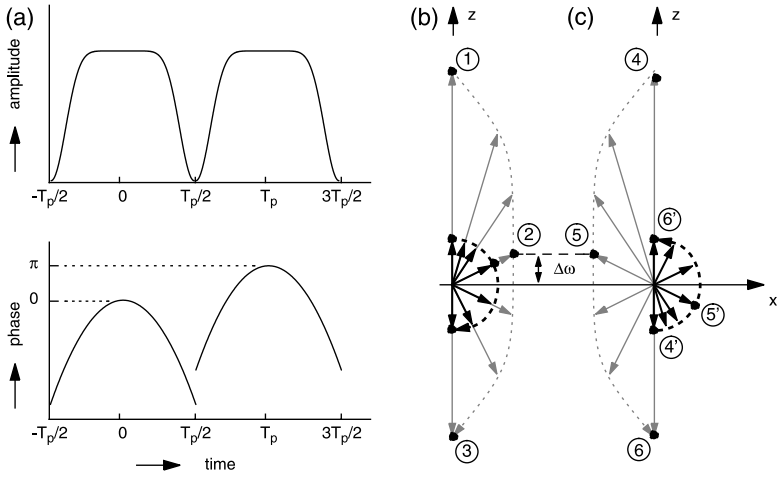

Fig. 2. (a) Amplitude and phase modulation scheme of the C element. The C element consists of two adiabatic inversion pulses which are identical except for an overall phase shift by π. Each pulse is furthermore symmetric about its center. The phase is given in a frame rotating at a fixed frequency (the RF frequency at the center of each pulse), the "PM frame." (b) Variation of the effective field (grey) and the polarization (black) in the course of the first pulse, in a frame rotating with the RF (the "FM frame"). The polarization is locked along the effective field as long as the adiabatic condition is fulfilled. (c) During the second pulse, the polarization is locked along the negative effective-field direction and returns to its initial state along the z-axis.

For obtaining an estimate of the minimum possible pulse length, the adiabaticity parameter $Q = \omega_{\text{eff}}/\dot{\theta}$ provides a good guideline, where ω_{eff} is the effective field in angular frequency units and $\dot{\theta}$ is the time derivative of the angle between the effective-field and the RF-field directions. The adiabaticity parameter varies with time in the course of a sweep, and it depends on the CS offset $\Delta\omega$ (i.e., the difference between the RF frequency at the center of the sweep, $t = 0$, and the resonance frequency of the spin). The parameter Q_0 in Eq. (4) is the adiabaticity at $t = 0$ for spins without CS offset: $Q_0 = Q(t = 0; \Delta\omega = 0)$. We wish to determine, for a given peak RF amplitude $\omega_1^{\max}$, the minimum pulse length T_p for which the adiabaticity of all spins within a given bandwidth of $\Delta\omega$ stays above a certain minimum value; a minimum adiabaticity of about 5 is reputed to lead to a "good" inversion. The relevant bandwidth is about 30 kHz for ^{13}C nuclei (~200 ppm CS range) at 150 MHz Larmor frequency. In order to achieve a global minimum of the adiabaticity of 5 within this bandwidth with a reasonable RF amplitude of, say, $\omega_1^{\max}/(2\pi) = 70$ kHz, our calculations show that the minimum required pulse length is about 45 μs for a WURST-8 pulse. This leads to a minimum cycle time of about 90 μs for a single WiW cycle and 810 μs for a complete WiW9_n^1 supercycle.

We wish to add two remarks: First, by a suitable (numerical) optimization, adiabatic pulses may be found that achieve a higher global minimum of the adiabaticity for a given pulse length than the simple WURST pulses. However, this is not the key concern of this paper. Second, while the adiabaticity parameter gives a good guidance in constructing or selecting a suitable pulse shape, a much better criterion is the simulated performance of the pulse, either with respect to single-spin inversion or with respect to the polarization transfer achievable with a TOBSY sequence constructed from such pulses, in the presence of anisotropic interactions under MAS. This issue will be addressed next.

3.3. Simulations

For numerically assessing the performance of a typical adiabatic inversion pulse, we simulated the single-spin inversion by WURST-8 pulses, varying the maximum RF amplitude $\omega_1^{\max}$ and the resonance offset $\Delta\omega$. The pulse length was set to $T_p = 50$ μs, and a frequency sweep range from −137 to +137 kHz (corresponding to $Q_0 = 5$ for $\omega_1^{\max}/(2\pi) = 66$ kHz) was used. A MAS frequency of 20 kHz was assumed. For RF amplitudes above 61 kHz, the simualtions yielded expectation values of I_z that were lower than −0.99 (i.e., the inversion was better than 99.5%) for CS offsets up to 15 kHz. This result is in good agreement with the above estimates obtained by regarding the adiabaticity parameter. We can conclude that, even if some B_1 inhomogeneity on the scale of ±10% is taken into account, a good, broadband single-spin inversion by pulses of 50 μs duration can be expected for nominal peak RF-field amplitudes of above approximately 70 kHz.

For the following simulations of polarization transfer by a complete TOBSY sequence, we fixed the duration of the WURST-8 pulses to 50 μs. The polarization transfer expected for the sequence WiW9_n^1 was simulated as a function of the mixing time and the RF amplitude of $n = 15$, 21, 24, 30, 33, and 39. Because of the fixed relationship between MAS frequency and pulse length due to rotor synchronization, the corresponding MAS frequencies were 16.67, 23.33, 26.67, 33.33, 36.67, and 43.33 kHz, respectively. As a typical result, Fig. 3 shows the polarization transfer calculated for the WiW9_{21}^1 sequence at a MAS frequency of 23.33 kHz. For RF amplitudes between 64 and 70 kHz, an oscillatory transfer efficiency as a function of the mixing time is obtained with a maximum transfer, in the powder average, of more than 90%. The large tolerance with respect to the setting of the RF amplitude is a dramatic improvement over the P9_6^1 sequence with hard pulses, where in the analogous simulation the transfer dropped close to zero for deviations of the RF amplitude by more than 5% from the nominal value [4]. The first maximum occurs after about 15 ms, instead of the $(2J)^{-1} = 10$ ms that might be expected from the value of the J coupling used in the simulations. This scaling of the oscillation frequency occurs in the presence of chemical-shift differences between the two spins and is also observed with TOCSY in liquids [8]. It is a consequence of the fact that a spin whose chemical shift has the same sign as the

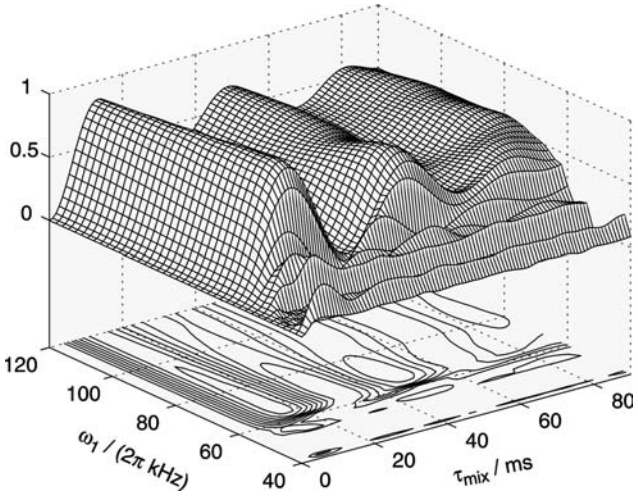

Fig. 3. Polarization transfer obtained in simulations of a two-spin system subjected to the WiW9_{21}^1 sequence at a MAS frequency of 23.33 kHz, as a function of the mixing time and the RF amplitude. Contour levels are drawn in 10%-steps between 20 and 90% of the initial polarization. For all RF amplitudes above 64 kHz, an oscillatory transfer with a maximum transfer of more than 80% is obtained. This is a consequence of the insensitivity of adiabatic pulses to RF inhomogeneity.

intial offset of the inversion pulse is inverted earlier than a spin whose chemical shift has the opposite sign (cf. Fig. 2). In other words, in a Bloch vector picture, the two polarizations corresponding to the two spins have an angle between them that is different from zero, which leads to the scaling of the coupling between them.

For the other values of n (with corresponding MAS frequencies), similar results were obtained. In general, the higher the MAS frequency, the less the oscillation of the transfer curve is damped. On the other hand, the RF amplitude threshold above which a "high" (>80%) transfer is achieved increases from 62 to 82 kHz with the MAS frequency increasing from 16.67 kHz ($n = 15$) to 43.33 kHz ($n = 39$).

For $\mathrm{WiW9}^{1}_{15}$, $\mathrm{WiW9}^{1}_{21}$, and $\mathrm{WiW9}^{1}_{24}$, the transfer curves were also simulated with a fixed RF amplitude of 66 kHz as a function of the length of a single WURST inversion pulse in the sequence (and consequently, of the MAS frequency). An oscillatory transfer with a maximum of over 80% was generally obtained for variations of the pulse length (and thus of the MAS frequency) in the ±10% range, keeping the amplitude/phase definition of the pulse unchanged. These ranges can be still widened by changing the maximum amplitude and/or the frequency sweep range of the pulses. Thus, the $\mathrm{WiW9}^{1}_{n}$ sequences are expected to be applicable in a wide range of MAS frequencies.

The simulated susceptibility of the $\mathrm{WiW9}^{1}_{24}$ sequence to resonance offsets is shown in Fig. 4. The maximum transfer is plotted as a function of the CS offsets of the two resonances for an RF amplitude of 66 kHz and a MAS frequency of 26.67 kHz. A square delimits the region where the chemical shifts are within a range of ±10 kHz. Along the diagonal, i.e., for off-resonance irradiation without CS differences, the region of high (>80%) transfer extends far outside this region, from offsets of −19 to +19 kHz. Along the antidiagonal, however, i.e., for irradiation at the center of two symmetrically shifted resonances, the maximum transfer remains above 80% only for CS differences of up to 16 kHz and decreases rapidly to a value of 20% for a CS difference of 20 kHz. Thus, the sequence becomes quickly inefficient for large CS differences. For the RE field assumed in this simulation (66 kHz), the bandwidth is just sufficient to promote transfer between a carbonyl and a C^{α} carbon in a polypeptide at a field of 14 T. The bandwidth can be improved by increasing the RF amplitude: Simulations with a maximum RF amplitude of 132 kHz yielded a transfer of more than 80% for CS differences up to 22 kHz.

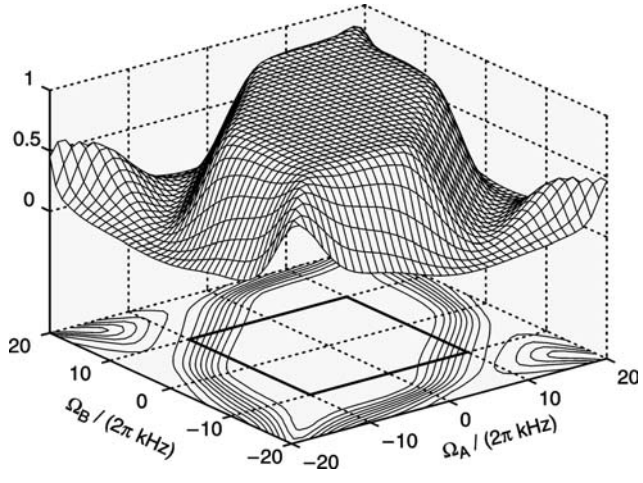

Fig. 4. Maximum transfer obtained in simulations using the $\mathrm{WiW9}^{1}_{24}$ sequence as a function of the CS offsets of the two resonances. The RF amplitude was 66 kHz, the MAS frequency 26.67 kHz. Contour levels are drawn in 10%-steps between 10 and 90% of the initial polarization. A square delimits the region where the chemical shifts are within a range of ±10 kHz.

Similar simulations were performed for a number of different pulse definitions, including MIP [22], CAP [27], ca-WURST [28], tanh/tan [29], and sech/tanh [30] pulses. The results were either comparable or somewhat inferior to those obtained with the WURST shapes, showing that the exact amplitude and phase definition of the pulse are of only limited influence for the performance if reasonable parameters are chosen.

4. Experimental characterization of the sequence $\mathrm{WiW9}^{1}_{24}$

4.1. Two-spin systems

Fig. 5a shows the dependence of the transferred polarization on the mixing time for [2,3-$^{13}C_2$]sodium propionate, using the $\mathrm{WiW9}^{1}_{24}$ sequence at a MAS frequency of 26.67 kHz. WURST-10 pulses were used as building blocks of the sequence. Before the start of the TOBSY sequence, polarization was created solely on the methyl ^{13}C spins, $I^{\Sigma}_{0} = I^{CH_3}(0)$. The mixing sequence then transfers polarization to the methylene ^{13}C spins. The transferred polarization after the mixing sequence is plotted in units of the initial total polarization: $I^{CH_2}(t)/I^{\Sigma}_{0}$. In addition, the sum polarization $I^{\Sigma}(t)/I^{\Sigma}(0) = (I^{CH_3}(t) + I^{CH_2}(t))/I^{\Sigma}_{0}$ is plotted. The transferred polarization exhibits an oscillatory behavior. A maximum transfer of 76% was obtained after 13.5 ms. The mixing time at which the maximum occurred is in good agreement with the $(2J)^{-1} = 13.9$ ms expected from the solution value of $J = 36$ Hz; as the isotropic CS difference of the involved spins is small (18.5 ppm or 2.8 kHz), no scaling of the oscillation frequency occurred. For comparison, also the transfer curve for the non-adiabatic $\mathrm{P9}^{1}_{6}$ sequence is shown. Here, a maximum transfer of only 46% was achieved, despite a careful optimization of the relevant parameters.

In these experiments, the peak RF amplitude of the adiabatic WURST pulses was 90 kHz. In many applications, the *average* power deposited in the sample

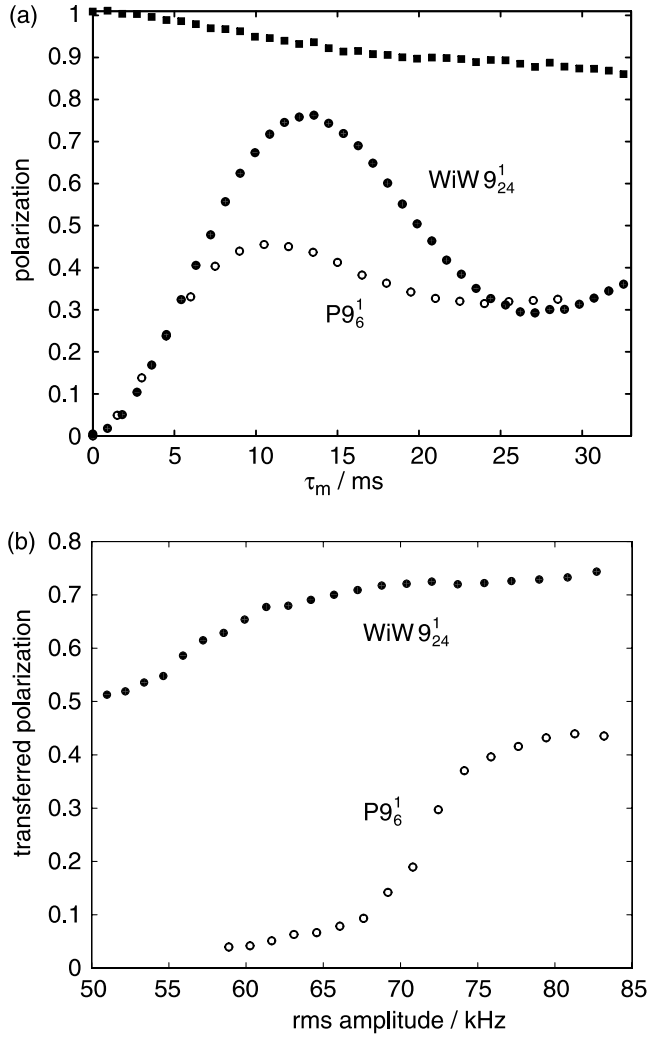

Fig. 5. Polarization transfer from the methyl to the methylene ^{13}C spins in [2,3-$^{13}C_2$]sodium propionate using two different TOBSY sequences at a MAS frequency of 26.67 kHz. (a) Dependence on the mixing time. For the WiW9$^1_{24}$ sequence, both the sum polarization (squares) and the transferred polarization (circles) are shown. A maximum transfer of 75% was obtained. This is significantly more than for the P9$^1_6$ sequence (open circles), for which a maximum transfer of 46% was observed. (b) Dependence on the RF amplitude at a mixing time of 12.6 ms (WiW9$^1_{24}$) and 12.38 ms (P9$^1_6$), respectively. The transferred polarization is shown as a function of the rms amplitude, which for the adiabatic WURST-10 pulses employed in the WiW9$^1_{24}$ sequence amounts to 83% of the maximum amplitude. In addition to a much higher transfer efficiency, the WiW9$^1_{24}$ sequence (closed circles) shows a much improved tolerance to the RF amplitude setting than the P9$^1_6$ sequence (open circles).

during the mixing sequence rather than the *peak* amplitude is of concern. It is thus often more appropriate to state the value of the root mean squared (rms) amplitude, i.e., the amplitude of a ficticious square pulse of same length with equal energy deposition in the probe. For the WURST-10 pulses used here, the rms amplitude amounts to 84% of the peak amplitude, or 76 kHz. This is slightly less than the RF amplitude of the P9$^1_6$ sequence, which is 80 kHz.

The dependence of both the WiW9$^1_{24}$ and P9$^1_6$ sequences on the RF amplitude was further investigated by varying the rms RF amplitude for a fixed mixing time close to the value for maximum transfer. The results are shown in Fig. 5b The WiW9$^1_{24}$ sequence exhibits a very favorable dependence on the RF amplitude. Almost uniform polarization transfer of more than 70% is obtained for rms values of the RF amplitude above 66 kHz. This highly uniform transfer efficiency will be especially favorable in cases where a large RF inhomogeneity is present. In contrast, the transfer efficiency of the P9$^1_6$ sequence drops rapidly below 20% for deviations of the RF amplitude by more than about 10% from the nominal value required by rotor synchronization (80 kHz).

For avoiding a fast decay of the sum polarization, efficient proton decoupling during the mixing time was found to be mandatory for the TOBSY sequences. During decoupling, Hartmann–Hahn conditions between the ^{13}C and the ^1H channels which might lead to undesired polarization transfer into the proton system must be avoided. It was found in our experiments that a good transfer efficiency could be achieved by off-resonance cw irradiation of the protons [31]. The optimum offset leading to maximum transfer was determined experimentally and was found to be generally somewhat larger than the offset required for Lee–Goldburg homonuclear decoupling for the WiW9$^1_{24}$ sequence (190 kHz offset at 160 kHz RF amplitude).

The same experiment was repeated for doubly ^{13}C-labelled zinc acetate. The CS difference between the methyl and carboxyl ^{13}C spins in a 14 T field is rather large, amounting to 24.6 kHz. As predicted by the simulation in Fig. 4, the maximum transfer obtained was low, amounting to only 15% (results not shown). For comparison, the transfer curve was also measured at 7 T on a Chemagnetics CMX-300 spectrometer with the WiW9$^1_{21}$ sequence at a MAS frequency of 23.33 kHz. An oscillatory transfer with a maximum of 55% was obtained (results not shown). The maximum occurred after a mixing time of 12.6 ms, which is well above the 9.6 ms expected from the J coupling in zinc acetate, which is $J = 52$ Hz (measured on a dissolved sample). Thus, as predicted by the simulations, a scaled J coupling is observed in the experiments because of the relatively large CS difference of 12.3 kHz.

Fig. 6 shows the dependences of the transfer efficiency as well as of the sum polarization on the synchronization of the pulse sequence with the MAS rotation. For a fixed timing of the WiW9$^1_{24}$ pulse sequence, with a pulse width of $T_p = 50\,\mu s$, the MAS frequency was varied around the value of 26.67 kHz, for which the pulse sequence is correctly synchronized with MAS. Both the transferred polarization and the sum polarization show similar dependences: Regions of good transfer efficiency and high sum polarization are interrupted by minima where

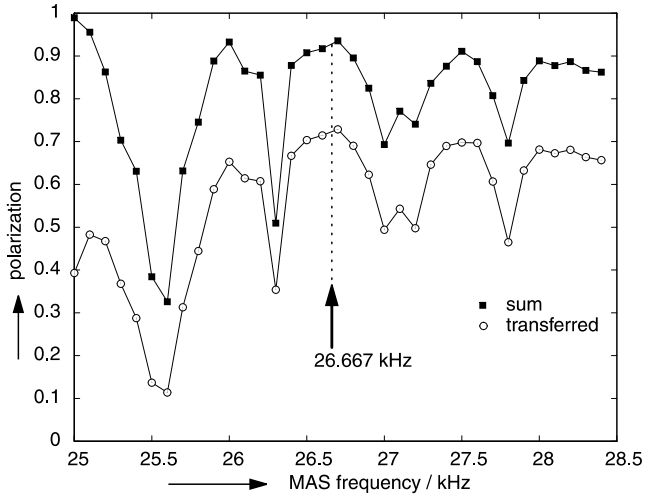

Fig. 6. Effect of deviations from synchronization of the pulse sequence with the MAS rotation. The transferred polarization (circles) and the sum polarization at the the end of the sequence (filled squares), relative to the intial polarization, were determined as a function of the MAS frequency under a $WiW9^1_{24}$ sequence with $T_p = 50\,\mu s$, which is synchronized correctly at a MAS frequency of 26.67 kHz (arrow). The mixing time was kept constant at 12.6 ms. Lines are added between data points to guide the eye. The sequence is insensitive to missettings of the MAS frequency on the scale of ~100 Hz. For larger missettings, minima occur in both the transferred and the sum polarization.

the transfer efficiency is compromized and the sum polarization decays rapidly under the pulse sequence. In the vicinity of the "correct" MAS frequency of 26.67 kHz, the pulse sequence is insensitive to synchronization errors on the scale of 100 Hz; this makes the sequence very robust to small fluctuations of the MAS frequency as are sometimes experienced in practice. For larger differences, the performance degrades rapidly to local minima. These minima correspond to synchronized $WiWN^v_n$ sequences with different values of N, n, and/or v. By the way of example, the deep minimum at a MAS frequency of 25.55 kHz corresponds to a synchronized $WiW9^1_{23}$ sequence. This sequence recouples parts of the dipolar and CSA interactions, which explains the strong decay of the sum polarization under the sequence. Between these minima, the transfer efficiency can be as high as for the correctly synchronized $WiW9^1_{24}$ sequence. This can be regarded as a consequence of the fact that—unlike dipolar recoupling sequences—a TOBSY pulse sequence does not need to reintroduce any interactions which are averaged by MAS; its task is merely to suppress chemical shifts while not introducing any other interactions. As long as no conditions are met where CSA or dipolar interactions are recoupled, the sequence can be expected to fulfill this task, even if it is not rotor-synchronized in a particular way. A similar behavior has been previously seen in the context of decoupling with the XiX sequence, for similar reasons [18].

4.2. 2D spectroscopy of peptides

To illustrate the use of the TOBSY sequence for assignments, Fig. 7 shows a two-dimensional (2D) ^{13}C TOBSY spectrum of the uniformly ^{13}C,^{15}N-labelled

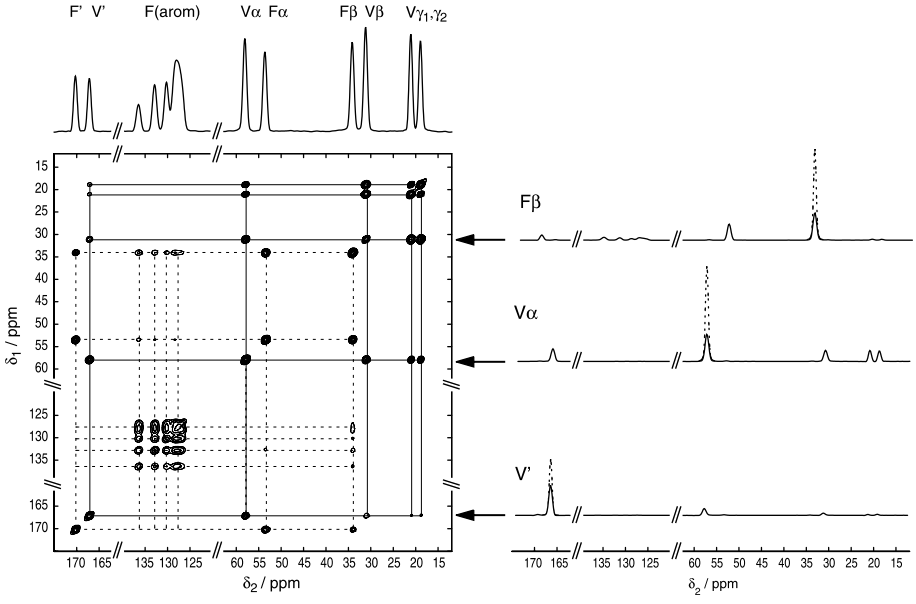

Fig. 7. Two-dimensional ^{13}C–^{13}C correlation spectrum of the dipeptide [U-^{13}C,^{15}N]L-Val–L-Phe obtained with the TOBSY sequence $WiW9^1_{24}$ at 26.67 kHz MAS frequency. On the top, the one-dimensional CP spectrum is shown together with the resonance assignments obtained from the two-dimensional correlation spectrum, shown below. Contours are at 2.5, 6.7, 14, 28, and 54% of the maximum intensity. The two spin systems can be clearly distinguished, as indicated by the solid and broken lines, respectively. At the right of the spectrum, 1D slices obtained by integrating along δ_1 over strips of 1.2 ppm are shown (solid curves) together with slices from a control spectrum with no mixing sequence applied (broken curves). From such strip projections, the transfer efficiency of the sequence was determined.

dipeptide L-Val–L-Phe. The $WiW9^1_{24}$ sequence was used at a MAS frequency of 26.67 kHz. The rms RF amplitude was 76 kHz (peak amplitude 90 kHz), the mixing time 10.8 ms. Two spin systems can be easily identified from the cross-peak pattern, each corresponding to the ^{13}C spins within one of the two amino acid residues. This leads immediately to the assignments indicated above the one-dimensional CP spectrum on the top of Fig. 7.

In order to assess the efficiency of the transfer within the spin systems, a control spectrum was recorded in which no mixing sequence was applied. In the right half of Fig. 7, 1D slices of the 2D spectra obtained with and without the mixing sequence are shown. These slices were generated by partially integrating the 2D spectrum along δ_1 in a strip of 1.2 ppm width centered around the resonance positions indicated by the arrows.

The top two slices illustrate the high transfer efficiency that can be achieved with the TOBSY sequence introduced here. In the middle slice, e.g., 55% of the polarization, initially localized on the C^α spin of the valine residue (at ~58 ppm), have been transferred into the cross-peaks. Cross-peaks are found from all spins in the valine spin system, enabling a complete assignment of this spin system.

The bottom slice, on the other hand, illustrates the somewhat limited bandwidth of the sequence. A relatively low transfer efficiency is observed due to the large isotropic CS difference between the carbonyl and the directly coupled C^α spin: Only 31% of the initial valine C' polarization is transferred to the cross-peaks.

In the average over all resonances, 54% of the initial polarization were transferred into the cross-peaks, with the sum polarization at the end of the mixing sequence amounting to 90% of the initial polarization. This high efficiency should make the sequence suitable for assignment studies in small amounts of labelled bioorganic materials.

Experiments were also performed on antamanide, cyclo-(Val–Pro–Pro–Ala–Phe–Phe–Pro–Pro–Phe–Phe), a cyclic decapeptide which has been extensively studied both in solution and in the solid state by a variety of methods. A 2D correlation spectrum was recorded with the same parameters as for the L-Val–L-Phe sample and with a mixing time of 12.4 ms. This spectrum is shown in Fig. 8. Again, intense cross-peaks are obtained which allow one to assign all amino-acid spin systems from this single spectrum. For determining the transfer efficiency, a control spectrum without mixing was recorded. Of the initial polarization determined in the control spectrum, 37% were transferred into the cross-peaks by the TOBSY sequence, while the total polarization decayed to 62%. Both values are improved over the results achieved with the $P9^1_{12}$ sequence on the same compound [13]. The decay probably reflects both the presence of large-amplitude motions in this system and imperfect proton decoupling.

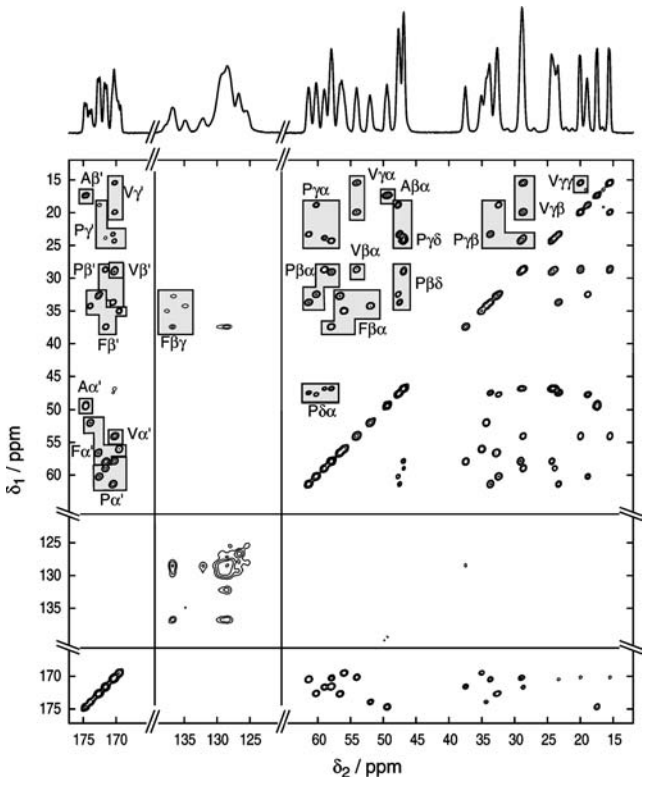

Fig. 8. Two-dimensional ^{13}C–^{13}C correlation spectrum of the cyclic decapeptide [U-^{13}C,^{15}N]antamanide. Parameters were the same as in Fig. 7, with contour levels at 2, 3.5, 6, 15, 30, and 70% of the maximum intensity. Intense cross-peaks allow one to readily assign the resonances in the spectrum to spin systems and amino acid types, as indicated.

4.3. Practical considerations

On first sight, the proposed pulse sequences may look rather complex and thus may seem to be difficult to set up. However, there is only a limited number of parameters involved which have to be adjusted. When setting up $WiW9^1_n$ sequences for ^{13}C–^{13}C transfer, we achieved good experimental results without additional optimization by adhering to the following considerations:

- The RF *amplitude shape* of the inversion pulses is of limited influence; good results were achieved with WURST-q pulses with amplitude exponents q between 2 and 10, higher exponents resulting in higher rms RF amplitudes, but better tolerance to RF inhomogeneities.
- The *pulse length* of a single inversion pulse and the *peak amplitude* are interconnected: The higher the amplitude, the shorter the pulse can be made without compromising the performance. Generally, the peak amplitude should be at least about 3.5 times the inverse of the pulse length. We achieved good results with pulses of about 50 μs length and peak RF amplitudes of at least about 70 kHz.

- For peak RF amplitudes in the range 70–90 kHz, a total frequency of 300–400 kHz generally gave good results.
- Proton decoupling is of great importance. Generally, the best results were achieved at the highest ^{1}H RF amplitudes tolerated by our probe (160 kHz). Off-resonance cw decoupling with a resonance offset slightly larger than the proton RF amplitude proved efficient.

None of the exact values of the above parameters are critical. The sequence tolerates rather large ranges of RF amplitudes and frequency sweeps. This makes the sequence easy to set up and robust to instrumental instabilities.

5. Conclusions

TOBSY sequences using adiabatic pulses were presented that achieve higher transfer efficiencies than previous TOBSY sequences and that are largely insensitive to RF inhomogeneities or instabilities. Suitable sequences can be found for almost any MAS frequency, including rapid MAS at frequencies above 40 kHz. In practice, setting the sequences up requires very little optimization.

Applications include resonance assignments in peptides and proteins. Despite the limited bandwidth of the tested sequence $WiW9^1_n$, all expected cross-peaks have been detected for the dipeptide L-Val–L-Phe at 14 T (600 MHz proton Larmor frequency). A correlation spectrum of the cyclic decapeptide antamanide suggests that the sequence is suitable for applications to larger biomolecular systems.

Acknowledgments

This work was financially supported by the ETH Zurich and Swiss National Science Foundation. One of the authors, E.H.H., thanks the Deutsche Forschungsgemeinschaft for a grant.

References

[1] L. Braunschweiler, R.R. Ernst, Coherence transfer by isotropic mixing: application to proton correlation spectroscopy, J. Magn. Reson. 53 (1983) 521–528.
[2] M. Baldus, B.H. Meier, Total correlation spectroscopy in the solid state. The use of scalar couplings to determine the through-bond connectivity, J. Magn. Reson. A 121 (1996) 65–69.
[3] A. Brinkmann, M.H. Levitt, Symmetry principles in the nuclear magnetic resonance of spinning solids: Heteronuclear recoupling by generalized Hartmann–Hahn sequences, J. Chem. Phys. 115 (1) (2001) 357–384.
[4] E.H. Hardy, R. Verel, B.H. Meier, Fast MAS total through-bond correlation spectroscopy, J. Magn. Reson. 148 (2001) 459–464.
[5] A.S.D. Heindrichs, H. Geen, C. Giordani, J.J. Titman, Improved scalar shift correlation NMR spectroscopy in solids, Chem. Phys. Lett. 335 (2001) 89–96.
[6] M. Hohwy, H.J. Jakobsen, M. Edén, M.H. Levitt, N.C. Nielsen, Broadband dipolar recoupling in the nuclear magnetic resonance of rotating solids: A compensated C7 pulse sequence, J. Chem. Phys. 108 (1998) 2686–2694.
[7] J.C.C. Chan, G. Brunklaus, R sequences for the scalar-coupling mediated homonuclear correlation spectroscopy under fast magic-angle spinning, Chem. Phys. Lett. 349 (2001) 104–112.
[8] Ē. Kupče, P. Schmidt, M. Rance, G. Wagner, Adiabatic mixing in the liquid state, J. Magn. Reson. 135 (1998) 361–367.
[9] W. Peti, C. Griesinger, W. Bermel, Adiabatic TOCSY for C,C and H,H J-transfer, J. Biomol. NMR 18 (2000) 199–205.
[10] Ē. Kupče, P.A. Keifer, M. Delepierre, Adiabatic TOCSY MAS in liquids, J. Magn. Reson. 148 (2001) 115–120.
[11] B. Heise, J. Leppert, R. Ramachandran, REDOR with adiabatic dephasing pulses, J. Magn. Reson. 146 (2000) 181–187.
[12] J. Leppert, B. Heise, M. Görlach, R. Ramachandran, REDOR: An assessment of the efficacy of dipolar recoupling with adiabatic inversion pulses, J. Biomol. NMR 23 (2002) 227–238.
[13] A. Detken, E.H. Hardy, M. Ernst, M. Kainosho, T. Kawakami, S. Aimoto, B.H. Meier, Methods for sequential resonance assignment in solid, uniformly ^{13}C, ^{15}N labelled peptides: quantification and application to antamanide, J. Biomol. NMR 20 (2001) 203–221.
[14] S. Hediger, B.H. Meier, R.R. Ernst, Adiabatic passage Hartmann–Hahn cross polarization in NMR under magic angle sample spinning, Chem. Phys. Lett. 240 (1995) 449–456.
[15] R. Verel, M. Baldus, M. Ernst, B.H. Meier, A homonuclear spin-pair filter for solid-state NMR based on adiabatic-passage techniques, Chem. Phys. Lett. 287 (1998) 421–428.
[16] R. Verel, M. Ernst, B.H. Meier, Adiabatic dipolar recoupling in solid-state NMR: The DREAM scheme., J. Magn. Reson. 150 (2001) 81–99.
[17] P. Tekely, P. Palmas, D. Canet, Effect of proton spin-exchange on the residual C-13 MAS NMR linewidths—phase-modulated irradiation for efficient heteronuclear decoupling in rapidly rotating solids, J. Magn. Reson. Ser. A 107 (2) (1994) 129–133.
[18] A. Detken, E.H. Hardy, M. Ernst, B.H. Meier, Simple and efficient decoupling in magic-angle spinning solid-state NMR: the XiX scheme, Chem. Phys. Lett. 356 (2002) 298–304.
[19] S. Smith, T. Levante, B.H. Meier, R.R. Ernst, Computer simulations in magnetic resonance. An object-oriented programming approach, J. Magn. Reson. A 106 (1994) 75–105.
[20] V.B. Cheng, H.H. Suzukawa, M. Wolfsberg, Investigation of a nonrandom numerical method for multidimensional integration, J. Chem. Phys. 59 (1973) 3992–3999.
[21] M. Edén, M.H. Levitt, Pulse sequence symmetries in the nuclear magnetic resonance of spinning solids: Application to heteronuclear decoupling, J. Chem. Phys. 111 (1999) 1511–1519.
[22] J. Baum, R. Tycko, A. Pines, Broadband and adiabatic inversion of a two-level system by phase-modulated pulses, Phys. Rev. A 32 (1985) 3435–3447.
[23] M. Garwood, K. Ugurbil, B1 insensitive adiabatic RF pulses, in: J. Seelig, M. Rudin (Eds.), NMR Basic Principles and Progress, Springer-Verlag, 1992, pp. 109–147.
[24] M. Garwood, L. DeLaBarre, The return of the frequency sweep: designing adiabatic pulses for contemporary NMR, J. Magn. Reson. 153 (2001) 155–177.
[25] Ē. Kupče, Applications of adiabatic pulses in biomolecular nuclear magnetic resonance, in: T. James, V. Doetsch, U. Schmitz (Eds.), Methods in Enzymology, vol. 338, Academic Press, 2001, pp. 82–111.
[26] Ē. Kupče, R. Freeman, Adiabatic pulses for wideband inversion and broadband decoupling, J. Magn. Reson. A 115 (1995) 273–276.

[27] D. Rosenfeld, Y. Zur, Is the sech/tanh adiabatic pulse really adiabatic?, J. Magn. Reson. 132 (1998) 102–108.
[28] Ē. Kupče, R. Freeman, Optimized adiabatic pulses for wideband spin inversion, J. Magn. Reson. A 118 (1996) 299–303.
[29] M. Garwood, Y. Ke, Symmetrical pulses to induce arbitrary flip angles with compensation for rf inhomogeneity and resonance offsets, J. Magn. Reson. 94 (1991) 511–525.
[30] M.S. Silver, R.I. Joseph, D.I. Hoult, Highly selective pi/2 and pi-pulse generation, J. Magn. Reson. 59 (1984) 34–3517.
[31] M. Baldus, B.H. Meier, Broadband polarization transfer in solid-state NMR: R/L schemes and their application to total through—space correlation spectroscopy, J. Magn. Reson. 128 (1997) 172–193.